GSA DATA REPOSITORY 2011175

Jansen et al., (2011), Does decreasing paraglacial sediment supply slow knickpoint retreat?

DR1. RELATIVE SEA LEVEL DATA

The most appropriate representation of river base level is mean tide level (MTL), which is the average of mean spring and mean neap tides. However, many relative sea level datasets are standardised to mean high water spring tides (MHWS), and because MTL and MHWS vary considerably between tidal stations in Scotland, palaeoshoreline elevations must be converted to an average height above MTL to reflect the precise magnitude of relative base level fall since shoreline abandonment. Smith et al. (2006) proposes Main Postglacial Shoreline isobases that for Loch Linnhe stand at 10 m MHWS, running along the southern shore from Fort William to Loch Etive. Relative tidal elevations at three Loch Linnhe tidal stations are given in Table DR1, and from these, the 10 m MHWS isobase converts to an average elevation of 12.2 ± 0.2 m OD (Ordnance datum, Newlyn), which amounts to 11.9 ± 0.2 m of relative base level fall. The elevation and abandonment ages of the Main Postglacial Shoreline (MPS), according to Smith (2006), is consistent with the relative sea level curve based on $^{10}Be_c$ ages on the emergent shoreline (Fig. 1C).

Table DR1. Sea-level data for tidal stations in Loch Linnhe (Admiralty Tide Tables, 2006).

	10 m MHWS (m)[1]	MTL (m)[1]	Loch Linnhe Main Postglacial Shoreline (m above MTL)
Corpach (Fort William)	12.02	0.27	11.75
Corran	12.44	0.37	12.07
Port Appin	12.25	0.45	11.80
mean ± 1 σ	12.24 ± 0.21	0.36 ± 0.09	11.87 ± 0.17

[1]Ordnance datum, Newlyn.

References

Admiralty Tide Tables, 1996, Volume 1: European waters including the Mediterranean Sea. Taunton. Hydrographer of the Navy.

Smith, D. E., Fretwell, P. T., Cullingford, R. A., and Firth, C. R., 2006, Towards improved empirical isobase models of Holocene land uplift for mainland Scotland, UK: Philosophical Transactions of the Royal Society A: 364, 949-972.

DR2. STREAM POWER DATA

The calculation of stream power per unit channel area (ω) in rivers Spean, Leven, Etive and Coe is based on: $\omega = \gamma.Q.S.W^{-1}$, where γ is the specific weight of water ($N.m^{-3}$), Q is water discharge ($m^3.s^{-1}$), S is channel slope and W is channel width (m). The specific gravity of water is assumed to be 9807 $N.m^{-3}$.

In Fig. 3B, modern local stream power per unit channel area was calculated from the pooled mean of 3 to 6 cross-sections along reaches between 20 and 50 m downstream from the knickpoint tip to the first $^{10}Be_c$ sample in each river (samples 5,15,18,22 in Fig. 2). Fig. 3B includes the uncertainty associated with each of the stream power variables: Q ±3.4 %, S ±10 %, and W ±20 %, giving a root mean square error of 22.6 %. Further details on each of the stream power variables are given below.

a) Discharge was calculated using a regional discharge-drainage area relationship. Flow data were analysed from nine flow gauges in the western Highlands with close to natural flow regime (i.e., natural to within 10% at or exceeding the 5-percentile flow). The study area receives a relatively uniform distribution of annual precipitation, and discharge with 0.5 annual exceedance probability ($Q_{0.5}$) is a linear function of drainage area (A in km^2), as given by $Q_{0.5}$ = 1.63 A + 7.19 (R^2 = 0.97). The $Q_{0.5}$ is assumed to be a reasonable representation of the channel-forming discharge, and based on this discharge-area relationship, $Q_{0.5}$ in the four rivers is calculated as follows: Spean, 1338 $m^3.s^{-1}$; Leven, 302 $m^3.s^{-1}$; Etive, 228 $m^3.s^{-1}$; and Coe, 97 $m^3.s^{-1}$.

b) The longitudinal channel bed profile was measured in the field with a differential global positioning system, producing a reach-slope uncertainty of ±10 %, and channel depth uncertainty of ±20 %.

c) Channel width was measured digitally from British Ordnance Survey 'Land-Line Plus' digital maps, which are available at two scales: 1:2500 (x,y relative uncertainty <1.8 m) and 1:10,000 (x,y relative uncertainty <4.0 m). Using Arc/Info, a channel centreline parallel to each bank was constructed with nodes at 10 m intervals, and channel width was measured at cross-sections drawn perpendicular to the banks at each node. The contributing drainage area at each cross-section was calculated by meshing the planimetric data with the NEXTMap digital elevation model (DEM), a 5m grid-scale map derived from airborne interferometric synthetic aperture radar (vertical accuracy RMSE = 1.0 m). Field channel width was measured perpendicular to banks using a laser range-finder or measuring tape. Channel width is defined by the limits of perennial vegetation, indicating the zone of active scour and/or mobile bed material, but more often the channel has two clear bedrock banks. Width measurement uncertainty is ±20 %.
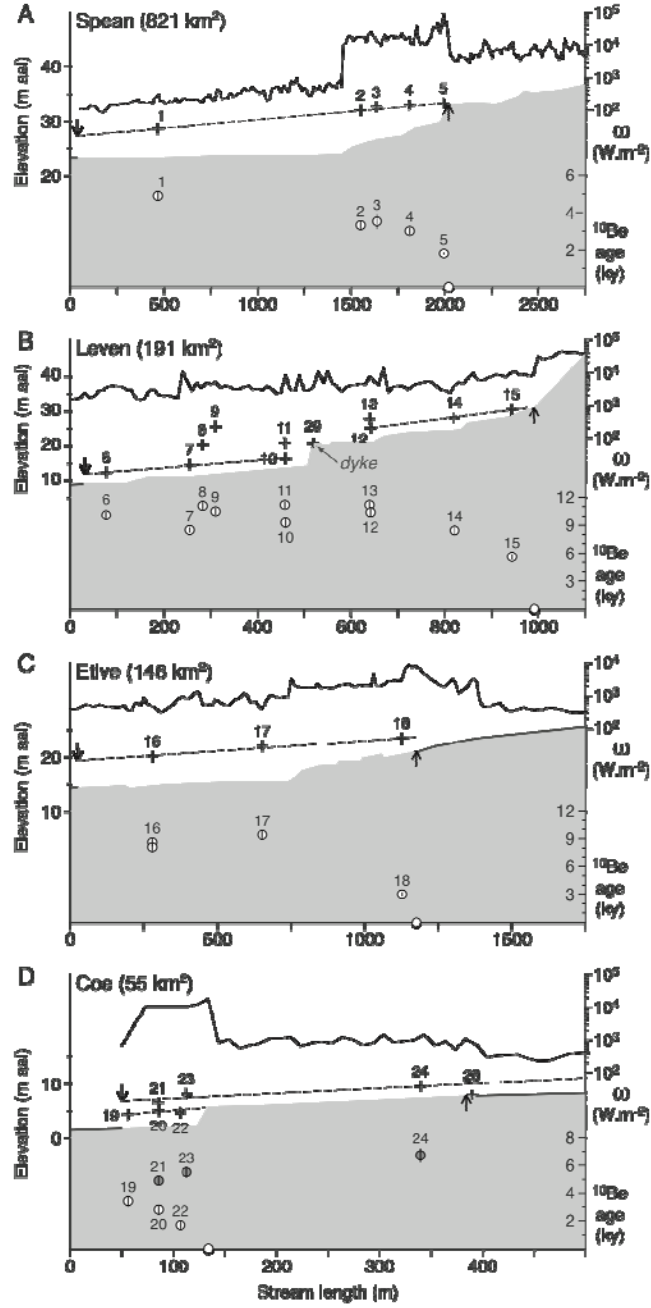
Figure DR1. Long profiles (grey shading), with strath terraces (dashes); [10]Be$_c$ samples (**+**) and [10]Be$_c$ ages (circles with verticals indicate ±1σ analytical uncertainty, and assume zero-age at knickpoint lips); and downstream variations in stream power per unit channel area (ω, black line). For ω calculations, average reach-slope is derived from a 100 m running-mean. [10]Be$_c$ samples (labels keyed to DR3) are plotted as zero-erosion exposure ages (ky), except samples 28 and 29, which, for reasons explained in the text, are modeled as maximum erosion rates (m.ky^{-1}). Down-arrow is initiation point of postglacial fluvial incision, up-arrow is retreating knickpoint, and thick gray line marks continuous alluvial bed cover. In B) the knickpoint has retreated to the base of a 30 m high waterfall formed in resistant metaquartz-arenite, and in D) [10]Be$_c$ ages from the emerged shoreline are shaded.

3

DR3. COSMOGENIC ANALYSES

Quartz cleaning and [10]Be extraction were done following standard procedures (Kohl and Nishiizumi, 1992; Child et al., 2000, Glasser et al., 2009) at the Glasgow Cosmogenic Isotope Laboratories (GCIL), and at the NERC Cosmogenic Isotope Analysis Facility (CIAF). The [10]Be/[9]Be ratios were measured with the 5MV accelerator mass spectrometer at SUERC (Freeman et al., 2004). Measurement is described in detail in Xu et al. (2010). The nominal ratios used for primary and secondary standards disagree with the re-calibration reported by Nishiizumi et al. (2007), however, the production rates are consistent with the ratios used in this work. Consequently, for the presented exposure ages (short compared to the half-life of [10]Be) only [10]Be concentrations reported here would be affected by implementing [10]Be/[9]Be ratios from Nishiizumi et al. (2007), and not the exposure ages. See Tables DR2A, DR2B, and DR2C, below (cf. Frankel et al., 2010).

References

Balco, G., Stone, J. O., Lifton, N. A., and Dunai, T. J., 2008, A complete and easily accessible means of calculating surface exposure ages or erosion rates from [10]Be and [26]Al measurements: Quaternary Geochronology, v. 3, p. 174-195.

Child, D., Elliott, G., Mifsud, C., Smith, A.M., and Fink, D., 2000. Sample processing for earth science studies at ANTARES: Nuclear Instruments and Methods in Physics Research B, v. 172, p. 856-860.

Dunne, J., Elmore, D., and Muzikar, P.F., 1999, Scaling factors for the rates of production of cosmogenic nuclides for geometric shielding and attenuation at depth on sloped surfaces: Geomorphology, v. 27, p. 3-11.

Frankel, K.L., Finkel, R.C., and Owen, L.A., 2010, Terrestrial Cosmogenic Nuclide Geochronology Data Reporting Standards Needed: Eos Transactions AGU, v. 91, p. 31-32.

Freeman, S.P.H.T., Bishop, P., Bryant, C., Cook, G., Fallick, A., Harkness, D., Metcalfe, S., Scott, M., Scott, R., and Summerfield, M., 2004, A new environmental sciences AMS laboratory in Scotland: Nuclear Instruments and Methods in Physics Research B, v. 31, p. 223–224.

Glasser, N.F., Clemmens, S., Schnabel, C., Fenton, C.R., and McHargue, L., 2009, Tropical glacier fluctuations in the Cordillera Blanca, Peru between 12.5 and 7.6 ka from cosmogenic [10]Be dating: Quaternary Science Reviews, v. 28, p. 3448-3458.

Hofmann, H.J., Beer, J., Bonani, G., Gunten, H.R. Von, Raman, S., Suter, M., Walker, R.L., Wölfli, W., and Zimmermann, D., 1987, [10]Be: Half-life and AMS-standards: Nuclear Instruments and Methods in Physics Research B, v. 29, p. 32-36.

Inn, K.G.W., Raman, S., Coursey, B.M., Fassett, J.D., and Walker, R.L., 1987, Development of the NBS [10]Be/[9]Be isotopic standard reference material: Nuclear Instruments and Methods in Physics Research B, v. 29, p. 27-31.

Kim, J. K., 2004, Controls over bedrock channel incision: Unpublished PhD thesis. Department of Geography and Geomatics, University of Glasgow, UK.

Kohl, C.P., and Nishiizumi, K., 1992, Chemical isolation of quartz for measurement of in-situ-produced cosmogenic nuclides: Geochimica et Cosmochimica Acta, v. 56, p. 3583-3587.

Middleton, R., Brown, L., Dezfouly-Arjomandy, B., and Klein, J., 1993, On [10]Be standards and the half-life of [10]Be: Nuclear Instruments and Methods in Physics Research B, v. 82, p. 399-403.

Nishiizumi, K., Imamura, M., Caffee, M.W., Southon, J.R., Finkel, R.C., and McAninch, J., 2007, Absolute calibration of [10]Be AMS standards: Nuclear Instruments and Methods in Physics Research B, v. 258, p. 403-413.

Xu, S., Dougans, A.B., Freeman, S.P.H.T., Schnabel, C., and Wilcken, K.M., 2010, Improved 10Be and 26Al-AMS with a 5 MV spectrometer: Nuclear Instruments and Methods in Physics Research B, v. 268, p. 736-738.

Yiou, F., and Raisbeck, G.M., 1972, Half-life of [10]Be: Physical Review Letters, v. 29, p. 372-375.

Table DR2A. Zero-erosion exposure ages for samples analysed at GCIL

Sample code[a]	Fig. 2 label	Lat (°)	Long (°)	Elevation (m asl)	Thickness[b] (cm)	Production Rate (atoms.g^{-1}.yr^{-1}) Spallation[c]	Muons[c]	Shielding Factor[d]	^{10}Be Concentration[e,f,g,h] (10^3 atoms.g^{-1} SiO$_2$)	Age[c,f,i] (ky)
SP-02/b2627	3	56.9039	-4.9679	31.0	2.25	4.21	0.182	0.9045	16.60 ± 1.92	3.5 ± 0.5
RL-04/b3338	12	56.7109	-4.9455	25.3	1.5	4.23	0.181	0.9092	49.18 ± 2.19	10.4 ± 0.5
RC-04/b756	19	56.6853	-5.0996	4.41	1.5	4.49	0.180	0.9883	16.95 ± 1.85	3.4 ± 0.5
RC-02/b750	20	56.6853	-5.0996	5.3	1.5	4.50	0.180	0.9883	14.05 ± 1.55	2.8 ± 0.3
RC-01/b1030	21	56.6853	-5.0996	6.4	2.25	4.47	0.180	0.9883	24.50 ± 1.68	4.9 ± 0.3
RC-09/b1966	22	56.6853	-5.0996	4.7	1.5	4.29	0.180	0.9441	7.94 ± 1.26	1.7 ± 0.3
RC-08/b1965	23	56.6853	-5.0996	8.2	1.5	4.55	0.180	0.9963	27.98 ± 2.07	5.5 ± 0.4
RC-05/b754	24	56.6853	-5.0996	9.6	1.5	4.52	0.180	0.9883	33.81 ± 2.46	6.7 ± 0.5
RC-03/b751	25	56.6853	-5.0996	2.4	1.5	4.49	0.180	0.9893	3.87 ± 1.17	0.8 ± 0.2
RC-10/b2507	27	56.6823	-5.0921	15.1	0.75	4.59	0.181	0.9943	46.10 ± 6.80	9.1 ± 1.3

[a] Sample codes denote rivers: Spean (SP), Leven (RL), and Coe (RC), and AMS code.
[b] The tops of all samples were exposed at the surface.
[c] Calculated with the CRONUS-Earth online calculator (Balco et al., 2008) version 2.1 (http://hess.ess.washington.edu/), using the time dependent Lal/Stone scaling scheme.
[d] Calculated according to Dunne et al. (1999).
[e] Isotope ratios were normalised to NIST SRM 4325 using ^{10}Be/^{9}Be = 3.06 x 10^{-11} (Middleton et al., 1993) and using a ^{10}Be half-life of 1.51 x 10^6 years (Yiou & Raisbeck, 1972; Hofmann et al., 1987; Inn et al., 1987).
[f] Uncertainties are reported at 1s confidence level.
[g] Corrected for a full chemistry procedural blank that yielded <3% of the number of ^{10}Be atoms in the samples.
[h] Propagated uncertainties include error in the blank, carrier mass (2%), and counting statistics.
[i] Propagated error in the model ages includes analytical uncertainty only with exception of samples 21,23,24,25, and 27 (the relative sea level curve data) for which the propagated error includes the total uncertainty.

Table DR2B. Zero-erosion exposure ages for samples analysed at CIAF

Sample code[a]	Fig. 2 label	Lat (°)	Long (°)	Elevation (m asl)	Thickness[b] (cm)	Production Rate (atoms.g^{-1}.yr^{-1}) Spallation[c]	Muons[c]	Shielding Factor[d]	^{10}Be Concentration[e,f,g,h] (10³ atoms.g^{-1} SiO$_2$)	Age[c,f,i] (ky)
SP-08/b3245	1	56.9082	-4.9816	28.7	1.5	4.56	0.182	0.975	24.62 ± 1.17	4.9 ± 0.2
SP-05/b3240	2	56.9038	-4.9690	32.0	1.5	4.58	0.182	0.9777	17.01 ± 0.92	3.3 ± 0.2
SP-06/b3241	4	56.9038	-4.9651	33.0	1.5	4.43	0.182	0.9428	14.96 ± 0.88	3.0 ± 0.2
SP-07/b3242	5	56.9029	-4.9627	33.3	1.5	4.39	0.182	0.9358	8.78 ± 0.69	1.8 ± 0.1
RL-09/b2639	6	56.7132	-4.9534	12.5	1.5	4.54	0.181	0.991	51.06 ± 2.07	10.1 ± 0.4
RL-11/b2652	7	56.7132	-4.9534	14.7	0.75	4.50	0.181	0.9725	42.62 ± 1.72	8.5 ± 0.3
RL-08/b2650	8	56.7127	-4.9504	20.4	1.5	4.44	0.181	0.9593	54.53 ± 2.27	11.1 ± 0.5
RL-10/b2641	9	56.7132	-4.9534	25.7	0.75	4.59	0.182	0.9799	53.36 ± 2.10	10.5 ± 0.4
RL-02/b2367	10	56.7119	-4.9480	16.4	2.25	3.91	0.181	0.8543	40.80 ± 2.60	9.3 ± 0.6
RL-01/b2342	11	56.7119	-4.9480	23.6	2.25	4.15	0.181	0.8993	51.76 ± 2.11	11.2 ± 0.4
RL-03/b2343	13	56.7110	-4.9457	20.2	3.0	3.88	0.181	0.8498	48.69 ± 1.94	11.2 ± 0.4
RL-05/b2344	14	56.7108	-4.9431	28.2	0.75	4.45	0.182	0.9488	41.38 ± 1.84	8.4 ± 0.4
RL-06/b2347	15	56.7108	-4.9411	30.6	1.5	4.48	0.182	0.9579	28.00 ± 1.54	5.6 ± 0.3
RE-03/b2640	16	56.5765	-5.0288	20.2	2.25	4.53	0.181	0.9869	43.23 ± 1.90	8.6 ± 0.4
RE-03'/b2648	16[j]	56.5765	-5.0288	20.2	2.25	4.53	0.181	0.9869	40.91 ± 1.94	8.1 ± 0.4
RE-04/b3239	17	56.5794	-5.0258	22.1	1.5	4.58	0.181	0.9894	47.93 ± 1.89	9.4 ± 0.4
RE-05/b3624	18	56.5830	-5.0230	23.5	1.5	4.57	0.181	0.9866	15.11 ± 0.78	3.0 ± 0.2
RC-06/b2348	26	56.6823	-5.0921	10.9	0.75	4.58	0.181	0.9943	42.15 ± 2.15	8.3 ± 0.4

[a] Sample codes denote rivers: Spean (SP), Leven (RL), Etive(RE), and Coe (RC), and AMS code.
[b] The tops of all samples were exposed at the surface.
[c] Calculated with the CRONUS-Earth online calculator (Balco et al., 2008) version 2.1 (http://hess.ess.washington.edu/), using the time dependent Lal/Stone scaling scheme.
[d] Calculated according to Dunne et al. (1999).
[e] Isotope ratios were normalised to NIST SRM 4325 using ^{10}Be/^{9}Be = 3.06 x 10^{-11} (Middleton et al., 1993) and using a ^{10}Be half-life of 1.51 x 10^6 years (Yiou & Raisbeck, 1972; Hofmann et al., 1987; Inn et al., 1987).
[f] Uncertainties are reported at 1s confidence level.
[g] Corrected for a full chemistry procedural blank that yielded <2% of the number of ^{10}Be atoms in the samples.
[h] Propagated uncertainties include error in the blank, carrier mass (2%), and counting statistics.
[i] Propagated error in the model ages includes analytical uncertainty only with exception of sample 26 (relative sea level curve data) for which the propagated error includes the total uncertainty.
[j] This sample was prepared and analysed twice (separate dissolutions).

Table DR2C. Samples modelled as maximum erosion rates

Sample code[a,b]	Fig. 2 label	Lat (^{o})	Long (^{o})	Elevation (m asl)	Thickness[c] (cm)	Production Rate (atoms.g^{-1}.yr^{-1}) Spallation[d]	Muons[d]	Shielding Factor[e]	^{10}Be Concentration[f,g,j] (10^3 atoms.g^{-1} SiO$_2$)	Erosion rate[d,g,k] (m.ky^{-1})
RC-07/b1964	28	56.6853	-5.0996	7.7	2.25	4.52	0.18	0.9963	19.86 ± 1.39[h]	0.24 ± 0.02
RL-07/b2649	29	56.7115	-4.9472	20.8	1.5	4.19	0.181	0.9055	20.34 ± 1.43[i]	0.23 ± 0.02
Etive-1[l]	–	56.6239	-4.9103	175	2.5	5.26	0.191	0.9748	50.30 ± 5.25	0.10 ± 0.01
Etive-2[l]	–	56.6239	-4.9103	172	2.5	5.24	0.191	0.9742	71.91 ± 6.52	0.07 ± 0.01

[a] Sample 28 analysed at GCIL, and sample 29 analysed at CIAF.
[b] Sample codes denote rivers: Leven (RL), and Coe (RC), and AMS code.
[c] The tops of all samples were exposed at the surface.
[d] Calculated with the CRONUS-Earth online calculator (Balco et al., 2008) version 2.1 (http://hess.ess.washington.edu/), using the time dependent Lal/Stone scaling scheme.
[e] Calculated according to Dunne et al. (1999).
[f] Isotope ratios were normalised to NIST SRM 4325 using ^{10}Be/^{9}Be = 3.06 x 10^{-11} (Middleton et al., 1993) and using a ^{10}Be half-life of 1.51 x 10^6 years (Yiou & Raisbeck, 1972; Hofmann et al., 1987; Inn et al., 1987).
[g] Uncertainties are reported at 1s confidence level.
[h] Corrected for a full chemistry procedural blank that yielded <3% of the number of ^{10}Be atoms in the samples.
[i] Corrected for a full chemistry procedural blank that yielded <2% of the number of ^{10}Be atoms in the samples.
[j] Propagated uncertainties include error in the blank, carrier mass (2%), and counting statistics.
[k] Propagated error in the model ages includes total uncertainty.
[l] Samples collected from the abraded Etive channel bed; analysed at Australian National University and reported in Kim (2004).

DR4. GRAIN SIZE DATA

Grain size was measured on large gravel bars formed close to the outlets of the four study rivers. One hundred grains were measured at each site following standard methods (Wolman, 1954). Median (d_{50}) grain sizes at the four sites span 90 to 260 mm, indicating readily transportable bed materials that are available as 'tools' for eroding bedrock.
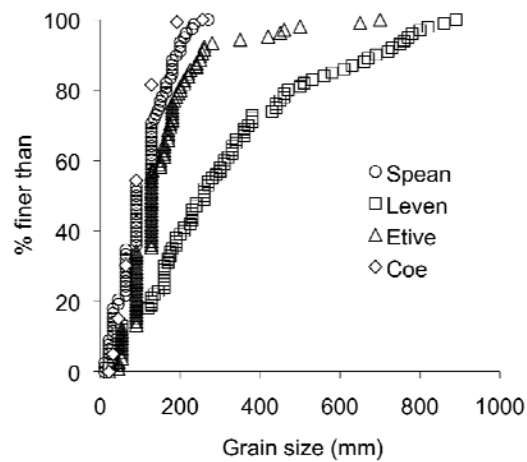

Figure DR2. Cumulative grain size frequencies for the four study rivers.

References

Wolman, M. G., 1954, A method of sampling coarse river bed-material: Transactions of the American Geophysical Union, v. 35, p. 951–956.

DR5. VOLUMETRIC RATES OF BEDROCK EROSION

The knickpoint retreat rate (V_{KP}) is converted to a volume of annual bedrock erosion below the knickpoint, as E = W.D.V_{KP}, where E is mean annual erosional flux ($m^3.y^{-1}$), W is channel width (m), and D is mean channel depth (m)(measurement details given in DR2). Uncertainties involved in our measurements: W ±20 %, and D ±20 %, yield a root mean square error of 28.3 %. Uncertainties associated with V_{KP} differ based on the $^{10}Be_c$ ages at each site, but full error propagation yields a root mean square error of 29–44 % for the estimates of erosional flux, as shown in Figs DR3 and DR4 below.
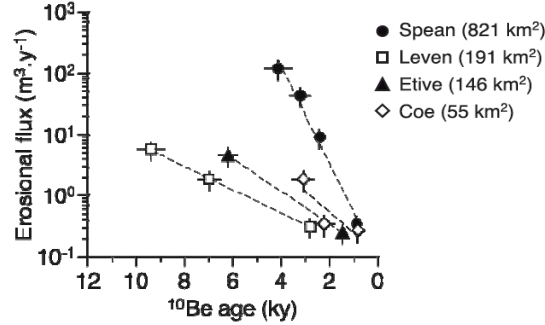

Figure DR3. Erosional flux versus $^{10}Be_c$ age, showing that erosional flux in the four rivers decreased sharply over the Holocene, and all have fallen to <0.4 $m^3.y^{-1}$ over the last 3 ky.
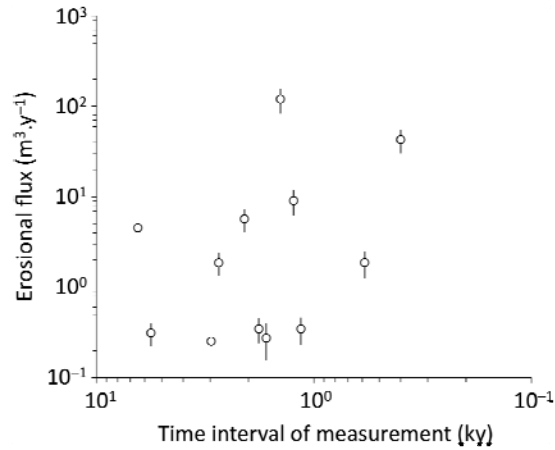

Figure DR4. Erosional flux versus time interval, showing no relationship exists between erosional flux and the time duration over which it is measured.